Marine Pollution Bulletin xxx (2012) xxx–xxx

Contents lists available at SciVerse ScienceDirect

Marine Pollution Bulletin

journal homepage: www.elsevier.com/locate/marpolbul

Linking coral river runoff proxies with climate variability, hydrology and land-use in Madagascar catchments

Joseph Maina [a,*], Hans de Moel [b], Jan E. Vermaat [b,c], J. Henrich Bruggemann [d], Mireille M.M. Guillaume [e,d], Craig A. Grove [f], Joshua S. Madin [a], Regina Mertz-Kraus [g,h], Jens Zinke [i,f]

[a] Department of Biological Sciences, Macquarie University, Sydney, NSW, Australia
[b] Institute of Environmental Studies, VU University, Amsterdam, The Netherlands
[c] Faculty of Earth and Life Sciences, Department of Earth Sciences and Economics, VU University, Amsterdam, The Netherlands
[d] Laboratoire d'Ecologie Marine (ECOMAR), Université de La Réunion, La Réunion, France
[e] Département Milieux et Peuplements Aquatiques, UMR CNRS-MNHN-UPMC-IRD BOrEA, Muséum National d'Histoire Naturelle, Paris, France
[f] NIOZ Royal Netherlands Institute for Sea Research, Department of Marine Geology, Texel, The Netherlands
[g] Max-Planck-Institut für Chemie, Mainz, Germany
[h] Berkeley Geochronology Center, Berkeley, CA, USA
[i] University of Western Australia Oceans Institute, School of Earth and Environment and Australian Institute of Marine Science, Perth, Australia

ARTICLE INFO

Key words:
Sedimentation
River discharge
Global climate change
Coral stress
Sclerochronology
Hydrological modeling
Land-use change
Ba/Ca
Luminescence

ABSTRACT

Understanding the linkages between coastal watersheds and adjacent coral reefs is expected to lead to better coral reef conservation strategies. Our study aims to examine the main predictors of environmental proxies recorded in near shore corals and therefore how linked near shore reefs are to the catchment physical processes. To achieve these, we developed models to simulate hydrology of two watersheds in Madagascar. We examined relationships between environmental proxies derived from massive *Porites* spp. coral cores (spectral luminescence and barium/calcium ratios), and corresponding time-series (1950–2006) data of hydrology, climate, land use and human population growth. Results suggest regional differences in the main environmental drivers of reef sedimentation: on annual time-scales, precipitation, river flow and sediment load explained the variability in coral proxies of river discharge for the northeast region, while El Niño-Southern Oscillation (ENSO) and temperature (air and sea surface) were the best predictors in the southwest region.

1. Introduction

The decline of coral reefs has been attributed to multiple and interacting global and local pressures. These pressures include pollutants from terrestrial sources (Gardner et al., 2003; Wilkinson, 2004), overfishing (Mora, 2010; Mumby et al., 2006), and changes in sea surface temperature (SST) and seawater pH (Eakin et al., 2009; Fabricius et al., 2011; Hoegh-Guldberg et al., 2007; Pandolfi et al., 2011). Coral reef ecosystem changes occur at different spatial scales, where local factors may exacerbate the effects of global processes, and temporal scales, where longer-term trends may be obscured by short-term, inter-annual and seasonal variability (Chabanet et al., 2005; Darling et al., 2010; Habeeb et al., 2005). Understanding the linkages between local and global processes in coastal watersheds and adjacent reef ecosystems is expected to lead to better coral reef conservation strategies (Jupiter, 2006; Prouty et al., 2010; Richmond et al., 2007). Furthermore, the development of long-term records of the physical environment of coastal watersheds, adjacent coral reef ecosystems, and linkages between them will help contextualize recent observations and help to identify the likely causes.

In Madagascar, several interacting environmental factors have changed over the past few decades, including air and sea surface temperature, storm frequency, rainfall quantity and intensity, soil erosion and sediment yield, river discharge, land cover, cropping systems, urbanization, coastal turbidity, and exploitation of reef fisheries (Alory et al., 2007; Hofmann et al., 2005; Kuleshov et al., 2008; Mavume et al., 2000; Zhang et al., 2007). For example, there has been extensive deforestation over the past 5 decades attributed to charcoal exploitation, cropland expansion, mining and increased logging (Harper et al., 2007; Sussman et al., 1994). The decline in forest cover is coincident with human population increase, loss of biodiversity in the forests (Ingram and Dawson, 2005; Hannah et al., 2008), and a significant decline in coral cover (Bruggemann et al., accepted for publication; Harris et al., 2010) over the same period. Long-term monitoring of environmental

* Corresponding author. Address: Department of Biological Sciences, Macquarie University, Sydney, 2109 NSW, Australia.
E-mail address: joseph.mbui@mq.edu.au (J. Maina).

0025-326X/$ - see front matter © 2012 Elsevier Ltd. All rights reserved.
http://dx.doi.org/10.1016/j.marpolbul.2012.06.027

change may provide early warnings of environmental regime shifts (Carpenter et al., 2011). Furthermore, a better understanding of environmental changes and how they interact may provide opportunities to change resource management practices and avoid irreversible and un-desirable ecological changes (Lindenmayer et al., 2011).

In Madagascar, long-term records of river discharge are sparse and the majority of sub-catchments are un-gauged. In such cases, hydrological models are required to provide spatial information for environmental management decision-making (Lu et al., 2006). Here we use STREAM hydrological model (Spatial Tools for River basins, Environment and Analysis of Management options; Aerts et al., 1999; Bouwer et al., 2006) and N-SPECT (Nonpoint-Source Pollution and Erosion Comparison Tool) (Eslinger et al., 2005) to reconstruct historical river discharge and sediment load in Madagascar catchments. STREAM is a grid-based spatial water balance model that describes the hydrological cycle of a drainage basin as a series of storage compartments and flows (Bouwer et al., 2006). Using monthly time step climate data as input, STREAM has successfully been applied in catchments of varying size in different parts of the world (e.g., Aerts and Bouwer, 2002; Bouwer et al., 2006).

Environmental proxy records, such as those laid down annually in the skeleton of massive *Porites* coral species, can augment model-based reconstructions and instrumental observations (Felis and Pätzold, 2003; Grottoli and Eakin, 2007; Prouty et al., 2010). We utilize two of these environmental proxies related to sediment load and river flow: the barium/calcium ratio (Ba/Ca; McCulloch et al., 2003) and the luminescence green/blue ratio (G/B; Grove et al., 2010), as indicators of environmental variability and long-term changes over the last five decades. Temporal variability of Ba/Ca in coral skeletons in near-shore areas has been shown to correspond with terrestrial sediment loading (Alibert et al., 2003; Lewis et al., 2011; Prouty et al., 2010). Barium (Ba) is dissolved into the drainage catchment and adsorbed to suspended sediments (clay minerals), which are then transported to coastal waters via rivers. As salinity increases, Ba desorbs from the suspended sediment due to the higher ionic strength of seawater. Ba diluted by seawater is thought to follow a conservative mixing pattern (Sinclair and McCulloch, 2004), and thus can act as a tracer for riverine sediment input into the ocean.

When placed under ultra-violet (UV) light, slices from inshore massive corals often display bright luminescent lines that have been linked to river flood plumes from coastal catchments and hence have the potential to provide a long-term record of hinterland precipitation (Isdale et al., 1998; Lough, 2011). Coral luminescence is thought to result from the incorporation of soil-derived humic acids transported to the reef during major flood events (Grove et al., 2010; Jupiter et al., 2008; Lough et al., 2002;). Here, we apply spectral luminescence scanning (SLS) of coral cores that uses the UV emission wavelength of the green (humic acid signal) relative to blue portions (skeletal density signal) of the electromagnetic spectrum, expressed as green/blue (G/B) ratio, as an indicator of the relative amount of humic acids in river runoff reaching the reef (Grove et al., 2010). Temporal variability in the Ba/Ca and G/B ratios (or luminescence intensity) has been successfully associated with a watershed's historical rainfall, erosion and river flow (Grove et al., 2010; Lough, 2011).

This study aims to evaluate the relationships between climate variables (i.e. air and sea surface temperature, precipitation, ENSO (El Niño-southern oscillation), population growth, land use change, hydrology, and coral core derived environmental proxies in the northeast (NE) and southwest (SW) Madagascar catchments. We develop hydrological models to reconstruct river discharge and sediment yield in these catchments and examine the relative importance of climatic versus anthropogenic processes as drivers of river flow and terrestrial sediment discharge. We test whether river discharge signals are recorded at the reef scale in Madagascar and discuss the validity of coral proxies as reliable recorders of environmental change. Further, we investigate evidence of change points or significant events, seasonality, and inter-annual and long-term trends in the time series of environmental and coral proxy data. We test the following hypotheses:

I. There is significant covariation between coastal climate, hydrology, land use (forest cover), population size and coral river runoff proxies.
II. Changes in coastal climate (precipitation, air and sea surface temperature), hydrology, forest cover, and population size significantly explain the variability in changes in coral river runoff proxies (i.e. Ba/Ca and G/B).

2. Methods

2.1. Study area

The island of Madagascar lies between 13°S and 25°S in the south-western Indian Ocean, extending roughly 1600 km in north–south direction and 500 km across. The western side is dominated by coastal plains and the transition between the west and the east coast plateaus consists of mountains >1500 m high. The east coast is wet and humid throughout the year, owing to orographic uplift of trade winds (Nassor and Jury, 1998). In the highlands the weather is determined by the dynamic interaction of trade winds, monsoon flow and the subtropical anticyclones, and a hot rainy season occurs during the Southern Hemisphere summer. Tropical cyclones and floods affect the NE and SW from November to May. The rainfall season starts in late December, with a convective peak in mid-February that declines by the end of March (Jury and Pathak, 1991). The cooler dry season occurs between June and October when climate is dominated by SE trade winds; it lasts up to 2 months longer in the SW of Madagascar compared to the NE. Annual total rainfall varies from 3700 mm in the east to 400 mm in the west and SW. Our study watersheds are located in the SW and in the NE. The Onilahy and Fiherenana rivers drain the SW watershed, while Antainambalana River, which flows into Antongil Bay drains the NE watershed (Fig. 1).

2.2. Hydrological modeling

Given the sparse observational long-term hydrological data for Madagascar, we employed STREAM to simulate monthly and annual river discharge patterns in the NE and SW regional watersheds (Aerts et al., 1999; Bouwer et al., 2006). STREAM simulates the water balance for each grid using a limited number of parameters, including spatial–temporal precipitation and temperature data, elevation, land-cover and soil water storage capacity (Aerts and Bouwer, 2002) (SI1 and SI2).

A configuration of the STREAM model was developed and run for the whole of Madagascar for 1950–2006. The model provided output time series of average monthly discharge in m^3/s for selected locations. These locations included outlet points of the Antainambalana and Onilahy Rivers, which drain the NE and SW watersheds, respectively, and eight gauging stations (Fig. 1), for which data were available in the RivDIS database (http://www.daac.ornl.gov/RIVDIS/rivdis.shtml) (Vorosmarty et al., 1998). The lengths of these records vary widely among stations. The Bevoay station on the Mangoky River had the longest time series (total of 310 months, intermittently between 1952 and 1994), and is relatively close to the SW watershed. Consequently, data from this station were used to calibrate the STREAM model by adjusting the various model coefficients to optimize the simulated

Please cite this article in press as: Maina, J., et al. Linking coral river runoff proxies with climate variability, hydrology and land-use in Madagascar catchments. Mar. Pollut. Bull. (2012), http://dx.doi.org/10.1016/j.marpolbul.2012.06.027

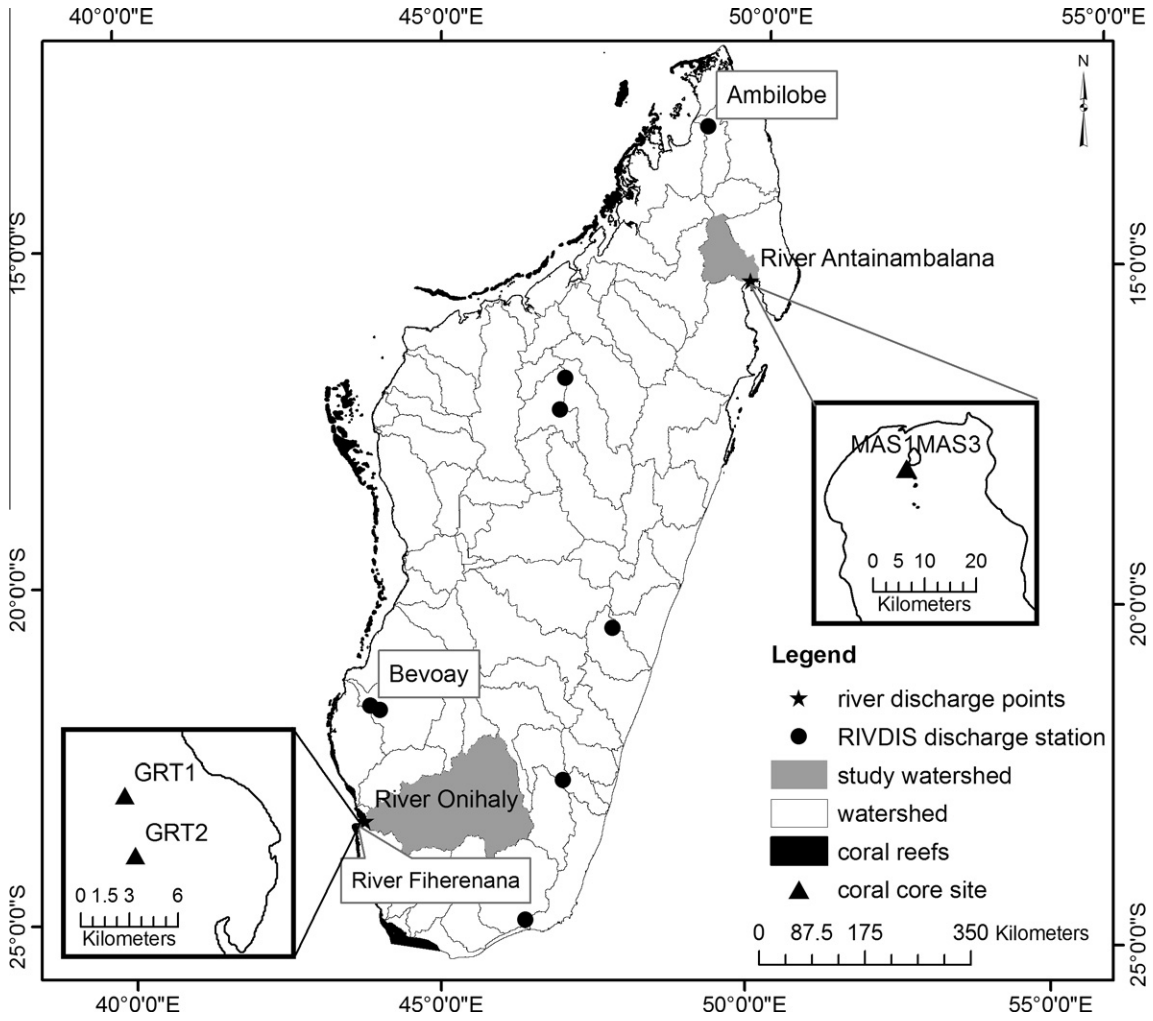

Fig. 1. Map of Madagascar showing all the watersheds, coral reefs, the northeast (NE) and southwest (SW) study basins, locations of the respective main rivers draining these basins, and river discharge observational stations (black filled dots). The location of the calibration (Bevoay) and validation stations (Ambilobe) for the hydrological model are indicated.

monthly hydrographs (Aerts et al., 1999). The performance of the model was tested at every stage using the model efficiency coefficient (NSE) (Nash and Sutcliffe, 2004), a widely used statistic in hydrological studies. NSE ranges between negative infinity and 1, where values between 0 and 1 are considered satisfactory, but values <0 indicate poor performance (see e.g., Moriasi et al., 2007). Respective discharge volumes were also compared by calculating the ratio of modeled to observed values. STREAM outputs were subsequently validated using the Ambilobe river discharge station in the north of Madagascar (Fig. 1).

Sediment yield per unit area was computed using the Non-Point Source Pollution and Erosion Comparison Tool (N-SPECT) developed by the National Oceanic and Atmospheric Administration (NOAA) (http://www.csc.noaa.gov/digitalcoast/tools/nspect/index.html). It combines data on elevation (Lehner et al., 2008), slope (Nam et al., 2003), soils (FAO/IIASA/ISRIC/ISSCAS/JRC, 2009), precipitation (Mitchell and Jones, 2005), rainfall erosivity (Vrieling et al., 2010), and land cover (Harper et al., 2007) to derive estimates of runoff, erosion, and pollutant sources (nitrogen, phosphorous, and suspended solids) from across the landscape, as well as estimates of sediment and pollutant accumulation in stream and river networks. The N-SPECT tool was run for each year from 1950 to 2006 to obtain estimates of annual sediment yield per unit area in mt/year (see SI1 and SI2 for details on input parameters).

2.3. Coral sampling and analysis

Coral cores were drilled in March and April 2007 from massive colonies of *Porites* spp. at water depths between 4 m and 6 m along the southern fringing reef slope at Nosy Mangabe Island in Antongil Bay (NE Madagascar) (Fig. 1) (Grove et al., 2010). Two of these cores (MAS1 and MAS3), drilled ~300 m apart and both located 7 km from the river Antainambalana's mouth, are utilized in this study. The river plume directly disperses towards the core sites, as described in detail in Grove et al. (2010). Two coral cores from SW Madagascar (GRT1 and GRT2) were drilled in March 2008 at 3 m depth on the inner slope of the *Grand Récif* of Toliara (GRT) (Fig. 1). The GRT, located <2 km seaward of Toliara town, is a major barrier reef system of the southwestern Indian Ocean. It stretches over 19 km (23°20–23°30S) between the Fiherenana River in the north and the Onilahy River in the south (Fig. 1) and represents approximately 33 km^2 of structurally diverse shallow reef area. Coral core GRT-1 is located 15.7 km north of the Onilahy river mouth and 11.2 km south of the Fiherenana River mouth, whereas GRT-2 is located 12.5 km north of the Onilahy River and 19.9 km south of the Fiherenana River.

A detailed description of the coral core sample preparation and analysis is given in Grove et al. (2010). In brief, coral cores were sectioned lengthwise into 7 mm thick slabs, rinsed several times

Please cite this article in press as: Maina, J., et al. Linking coral river runoff proxies with climate variability, hydrology and land-use in Madagascar catchments. Mar. Pollut. Bull. (2012), http://dx.doi.org/10.1016/j.marpolbul.2012.06.027

with demineralised water, blown with compressed air to remove any surficial particles and dried for more than 24 h in a laminar flow hood. Annual bands were visualised by X-radiograph-positive prints and luminescence imagery to produce an initial chronology based on annual density and luminescence bands (Grove et al., 2010). All coral slabs from the four cores were cleaned with sodium hypochlorite (NaOCl, 10–13% reactive chloride; Sigma–Aldrich Company) for 24 h to remove residual organics that might quench luminescence. Spectral luminescence scanning (SLS) was performed on bleached coral slabs using a line-scan camera fitted with a Dichroic beam splitter prism, separating light emission intensities into three spectral ranges: red (R), green (G) and blue (B) (Grove et al., 2010). We subsequently calculated the Green/Blue (G/B) ratio that reflects the changing humic acid/aragonite skeletal density ratio in the coral skeleton. To obtain Ba/Ca ratios at 40 μm intervals, slabs of the coral cores from NE Madagascar were analyzed by laser ablation inductively coupled plasma mass spectrometry (LA ICP-MS) at the Australian National University in Canberra, following the methods described by Fallon et al. (2002). We use 56 years (1950–2006) from the NE coral G/B and Ba/Ca data (cores MAS1 and MAS3). LA ICP-MS analyses on the SW Madagascar corals were done at the Max-Planck-Institut (MPI) für Chemie in Mainz (Germany). A detailed description of the LA ICP-MS procedure applied is given by Mertz-Kraus et al. (2009). Analysis in both laboratories utilized either NIST SRM 614 or 612 glasses as reference material. This approach has been shown to result in reliable, reproducible element concentrations in carbonate material (e.g., Fallon et al., 2002; Mertz-Kraus et al., 2009). Age models for both Ba/Ca and G/B ratios were based on the driest month in any given year (lowest Ba/Ca and G/B) in local rainfall and subsequent linear interpolation between the October anchor points using AnalySeries 2.0 (Paillard et al., 1996) to a monthly time scale (for details see, Grove et al., 2010). The G/B and Ba/Ca time series for the NE cover 1950–2006, and the Ba/Ca data for the SW cover 1976–2008 (GRT1) and 1975–2008 (GRT2).

2.4. Data analysis

Principal component analysis (PCA) was used to examine covariance and common temporal variations among hydrological variables (annual average discharge and sediment load), climatic variables (annual average sea surface temperature (hereafter SST), air temperature (hereafter AT), annual precipitation, the Niño3.4 SST anomaly index (i.e. an indicator of the strength of tropical Pacific ENSO events: http://www.cpc.ncep.noaa.gov/data/indices/), and the coral proxies for river flow and sediment load (G/B and Ba/Ca) from NE and SW watersheds. Given the temporal autocorrelation inherent in time series data, we used PCA to reduce the dimensionality of the data matrix by finding uncorrelated principal components (PCs) that together account for much of the variance in the original variables (Jackson, 2003, Jolliffe, 2004).

For each variable and watershed, time series data were aggregated on an annual basis using the November-October water year. For the NE, data for 11 variables were available in monthly time steps for 56 years (1950–2006) (SI2). For the SW, G/B data could not be used (see SI3); Ba/Ca time series were available at monthly time steps for 31 years (1976–2006). Consequently, for each region PCA was performed with seven environmental variables at 56 and 31 yearly time steps, respectively. PCA was repeated with the coral proxies, where four time series (two Ba/Ca and two G/B) and two time series (both Ba/Ca) were the input data for the NE and the SW, respectively. To estimate the association of each of the variables with the PCs, we performed pairwise correlations. To identify possible change points and their synchrony in the environmental multivariate and coral proxies time series, we applied the widely-used sequential *t*-test method (Rodionov, 2004) of environmental and coral proxies' PC's that explained >10% variability. A cut-off regime length of 10 years was chosen and default settings were used for the other parameters (probability = 0.1; Huber parameter = 1; no weighting). Bivariate plots of standardized absolute values of the environmental and coral proxies were also constructed.

To investigate the presence of seasonality in the time series, we used autocorrelation and present graphs showing correlations between values in a time series and those at a fixed time interval later (Davis, 1986). By investigating how a time series correlates with itself at different time lags, autocorrelation detects non-randomness in data using autocorrelation function, R (Box and Jenkins, 1976). An autocorrelogram is produced when the lags are plotted as a histogram at lags of $1, 2 \ldots t$. (Davis, 1986). The equations and methodology of autocorrelation function has been described in Chatfield (2004). For each variable, we also graphed the averaged absolute values for each month.

Finally, we employed generalized linear models (GLM) to determine which environmental variables explained the variability in coral runoff proxies in each watershed. Climate, land use, population and hydrologic variables were used as the predictors of coral proxies. Due to the temporal ordering of the data, pre-processing steps, i.e. *z*-score standardization and detrending, were carried out before fitting GLMs (Zuur et al., 2003). Detrending removes any temporal trend, which can be confounding and can lead to spurious relationships, while *z*-score standardizing ensures that the time series' statistical properties such as mean, variance, and autocorrelation are all constant over time. Because we were primarily interested in variables driving changes in coral proxies at yearly time-scales, we used first order differencing to detrend all *z*-score standardized time-series data.

Multicollinearity among predictor variables may have adverse effects on estimated coefficients in a multiple regression (Mansfield and Helms, 1982). To detect the existence of multi-collinearity in our data, variance inflation factors (VIF) were computed. VIFs specify how much of a regressor's variability is explained by the remaining regressors in the model due to correlation among those regressors (Cranet and Surle, 2002). A very conservative cut-off value of VIF = 3 was adopted relative to suggested values of 5 or 10 (Cranet and Surle, 2002). High multi-collinearity was detected due to high correlation between river flow, sediment load, and precipitation in both regions. Consequently these variables were used interchangeably in a model with uncorrelated variables.

Further, regression equations that use time series data often contain lagged variables (e.g., Zuur et al., 2003; Lui et al., 2007). In our context, lags may be due to uncertainties in the environmental data, hydrological models, alignment error in time series elements, dating of the environmental proxies, and time delays in biological processes (Barnes and Lough, 1993) among other factors, which could lead to temporal mismatch in data consequently concealing relationships. Therefore, we introduced 0–3 year lags ($Lag = t + 0 \ldots 3$) on predictor variables in the GLM process where GLM was repeated for each lag. For the NE, 4 models ($Lag = t + 0 \ldots 3$) were run three times (i.e. each time with precipitation, sediment load or river flow) for each response coral proxy data. Similarly, for the SW, 4 models were run three times for Ba/Ca. During the GLM stepwise process, predictor variables are added and dropped in several iterations until the best model is achieved based on the Akaike Information Criterion (AIC) model selection method (Zuur et al., 2009). To ensure robustness of the model estimates, residuals were examined for autocorrelation using the Durbin–Watson test (Durbin and Watson, 1971); no autocorrelation was found. We report only significant models in Table 2.

Please cite this article in press as: Maina, J., et al. Linking coral river runoff proxies with climate variability, hydrology and land-use in Madagascar catchments. Mar. Pollut. Bull. (2012), http://dx.doi.org/10.1016/j.marpolbul.2012.06.027

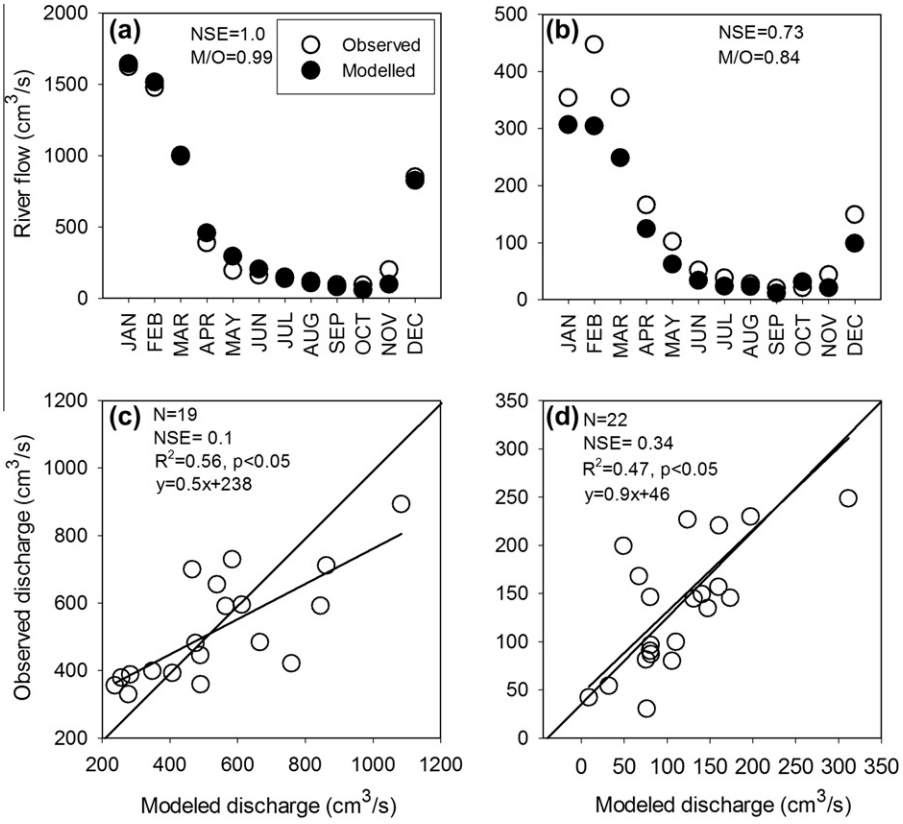

Fig. 2. Plots of observed against modeled discharge at monthly and annual aggregation levels at calibration and validation stations. Hydrograph and mean monthly average for each year for the calibration station (Bevoay, a and c), and for the validation station (Ambilobe, b and d) are shown. NSE index (see text) values and the model/observation ratio are presented, the latter is shown only for hydrographs. The regression line indicates the deviation of the modeled discharge relative to the diagonal line.

3. Results

3.1. Calibration and validation

Calibration of hydrological model (STREAM) results at Bevoay, based on 25 years of model simulation, are given in Fig. 2a and c. When simulations were compared with observed monthly averaged hydrographs of the respective catchments using the calibration tests (NSE and modeled/observed ratio), values were close to one, indicating good agreement. The validation of the annual hydrograph at Ambilobe (Fig. 2b and d) also shows good seasonal agreement. However the absolute amount of annual modeled discharge was slightly lower than observed (NSE- 0.73). Comparisons of observed/modeled annual discharges over time (Fig. 2, bottom panels) also revealed that the model performed well in both the calibration and validation stations with occasional mismatches in observed/modeled peak values (Fig. 2c and d). At Bevoay, the prediction at annual time scales was significant and explained a substantial part of the observed variance (56%), but the values of intercept (>0) and slope (<1), suggest a systematic discrepancy. Since we had no objective guidance to further adjust our model parameters, we accepted this difference: our model overestimates discharges above ~800 m^3/s.

3.2. Relationships among variables

PCA of environmental variables for the NE and SW revealed considerable covariance, with PC 1 and PC 2 in each region, together accounting for over 65% of the total variation in the multivariate samples (Table 1). In the NE, sediment yield, precipitation, river flow, forest cover, and population were highly correlated with PC 1 (39%) (Table 1) ($r \geqslant 0.6$). Also AT and SST correlated moderately ($r = 0.4$–0.5) with PC 1 and highly ($r \geqslant 0.6$) with PC 2 (29%). AT and SST covaried negatively with precipitation and with hydrological variables in PC 2. ENSO (Niño3.4 Index) correlated moderately with PC 1 and 2, and highly with PC 3 (15%) (Table 1), alongside forest cover, SST, and population growth. In the SW (Table 1), PC 1 (44%) was comprised mainly of temperature, population and forest cover, while PC 2 (30%) was comprised of precipitation, river flow and sediment load. PC 3 (12%) was highly correlated with ENSO ($r = 0.9$) and moderately with precipitation ($r = 0.2$). Comparisons of the PC's in the two regions indicate similarities and differences. Forest cover and population in both regions were highly prominent in PC 1. However, hydrological variables and precipitation associ-

Table 1
Correlation coefficients between leading three PCs for each region and various environmental and coral proxy time series. Bold values are statistically significant at the 95% confidence level.

Principal components	Northeast			Southwest		
	PC 1	PC 2	PC 3	PC 1	PC 2	PC 3
Contribution ratio (%)	39.4	29.3	15.1	43.7	30.4	11.6
Precipitation	**0.6**	**0.7**	**0.3**	0.0	**0.9**	**0.2**
Sediment load	**0.7**	**0.5**	−0.1	0.0	**0.8**	−0.1
River flow	**0.6**	**0.8**	**0.2**	−0.1	**1.0**	0.1
Forest cover	**−0.8**	**0.3**	**0.5**	**−0.9**	−0.1	0.1
Population	**0.8**	**−0.2**	**−0.5**	**0.9**	0.1	−0.1
Air temperature	**0.5**	**−0.7**	0.1	**0.9**	−0.1	−0.1
Sea surface temperature	**0.4**	**−0.6**	**0.4**	**0.9**	0.0	0.0
Niño3.4 index	**0.5**	**−0.4**	**0.6**	**0.3**	−0.1	**0.9**
Ba/Ca MAS1 (GRT1)	**0.6**	**−0.2**	**−0.3**	**0.4**	**0.2**	0.0
Ba/Ca MAS 3 (GRT2)	**0.3**	−0.1	**−0.3**	0.1	0.1	0.0
G/B MAS1	**0.6**	−0.1	**−0.2**			
G/B MAS 3	0.1	0.0	−0.1			

Please cite this article in press as: Maina, J., et al. Linking coral river runoff proxies with climate variability, hydrology and land-use in Madagascar catchments. Mar. Pollut. Bull. (2012), http://dx.doi.org/10.1016/j.marpolbul.2012.06.027

Table 2
Generalized linear model (GLM) outputs showing models that significantly explain the variation in each of the coral proxy variables in the NE and SW regions. GLM selects variables for deletion or inclusion based on Akaike Information Criterion (AIC)"; given a set of models for the data, the preferred model is the one with the minimum AIC value.

Dependent variable	Model AIC	Predictor	*t*-value	*p*
Northeast				
$Ba/Ca_{(t+2)}$	326	Precipitation	4.2	0.00
	327	Sediment load	3.2	0.00
	329	River flow	4.1	0.00
$G/B_{(t+0)}$	347	Air temperature	3.5	0.00
		Precipitation	1.9	0.05
		Niño3.4 index	−2.0	0.05
	349	Air temperature	3.59	0.00
		Sediment load	2.48	0.01
		Niño3.4 index	−1.85	0.07
	350	Air temperature	3.5	0.00
		River flow	1.7	0.095
		Niño3.4 index	−1.9	0.06
$G/B_{(t+2)}$	338	River flow	3.1	0.00
	338	Sediment load	3.1	0.00
	340	Precipitation	2.7	0.01
Southwest				
$Ba/Ca_{(t+1)}$	182	Air temperature	3.0	0.00
		Niño3.4 index	−3.5	0.00

ated with PC 1 in the NE were replaced by AT and SST in the PC1 in the SW.

Coral proxies, except G/B MAS 3, correlated highly with environmental PC 1, while Ba/Ca also correlated marginally with PC 3. For the SW, only one of the two Ba/Ca records (GRT1) correlated significantly with PC 1 and PC 2 (Table 1). For the NE, both proxies in MAS 1 highly (positively) correlated with PC1, while MAS3 Ba/Ca was moderately correlated with PC1. G/B and Ba/Ca in MAS1 were negatively correlated to PC2, which is mostly dominated by temperature, precipitation and river flow. Environmental proxies in both cores were also negatively associated with PC3, dominated mostly by ENSO, temperature, forest and land cover. For the SW, only one of the two Ba/Ca records (GRT1) correlated significantly with PC 1 (dominated by AT, SST, ENSO, forest cover and population growth). The same core showed significant but relatively lower correlation with SW PC2 (dominated by river flow, sediment load and precipitation, Table 1). These results suggest that precipitation and hydrology, both influenced by anthropogenic catchment alteration, are the key environmental drivers in the NE, but a significant contribution of temperature and ENSO is also evidenced. In the SW, forest cover, population growth, AT, SST and ENSO represent the main environmental drivers.

Change point analysis of environmental and coral proxies PCs for the respective regions revealed significant changes at various points in the time series (Fig. 3). In the NE, environmental PC 1

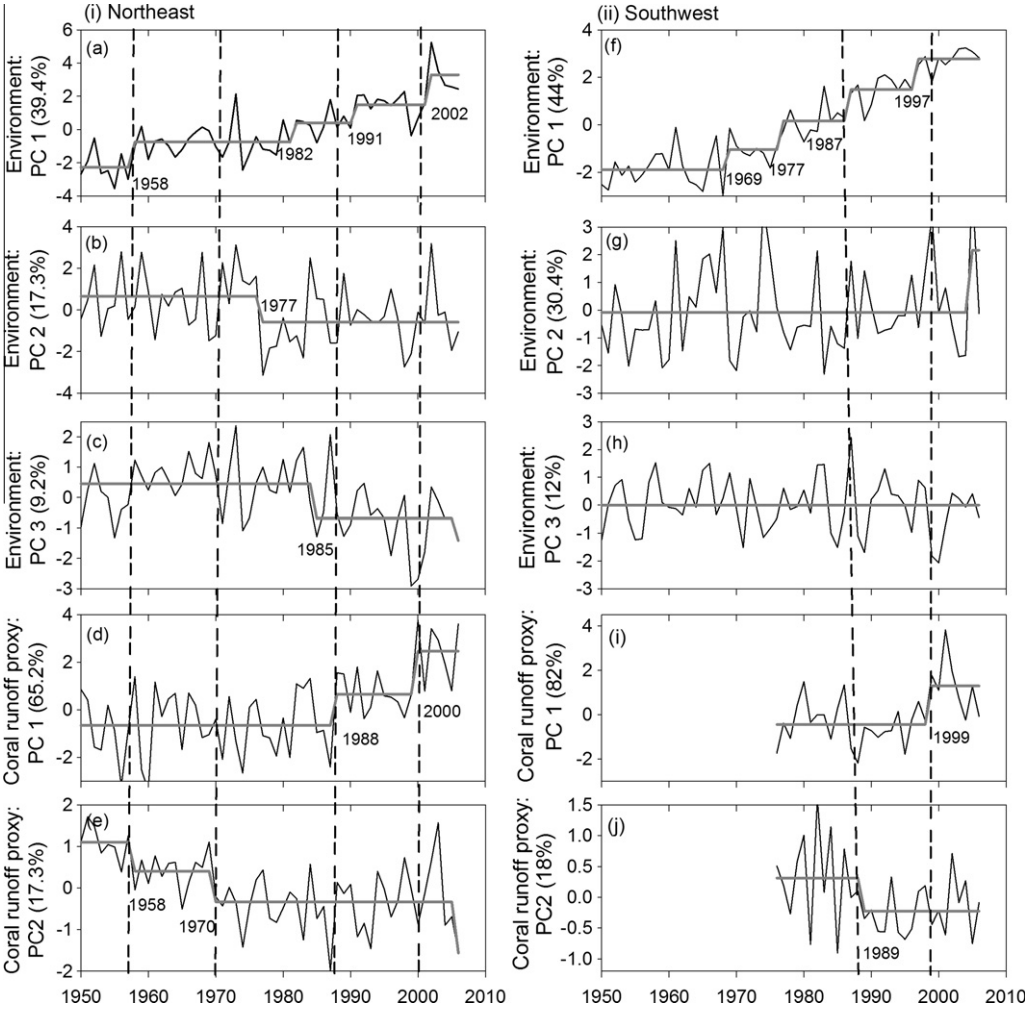

Fig. 3. Long term trend and change-point analysis of the first three principal components of the environment data time series (a, b, c, f, g, h); and of coral proxies for river flow and sediment load (d, e, i, j) with Rodionov's sequential *t*-test for (i) NE, and (ii) SW regions. The grey line indicates the regime and significance shifts are at $p < 0.01$, while the vertical dotted lines depict points of significant shifts in any of the PC's.

Please cite this article in press as: Maina, J., et al. Linking coral river runoff proxies with climate variability, hydrology and land-use in Madagascar catchments. Mar. Pollut. Bull. (2012), http://dx.doi.org/10.1016/j.marpolbul.2012.06.027

shows positive change points in 1958, 1982, 1991, 2002 (Fig. 3a). The 1991 and 2002 change points did approximately correspond, albeit with a lag of 2–3 years, with coral proxy PC 1 (65%), which showed positive shifts in 1988 and 2000 respectively (Fig. 3a and d). The 1958-change point appeared in both environmental parameters' PC 1 and coral proxies PC 2 (18%) (Fig. 3a and e). NE forest cover was negatively associated with environment PC 1, while the other variables were positively associated with PC1 (hydrology, precipitation, and population, Table 1). Thus, the stepwise change in hydrology, precipitation, and population growth reflects an

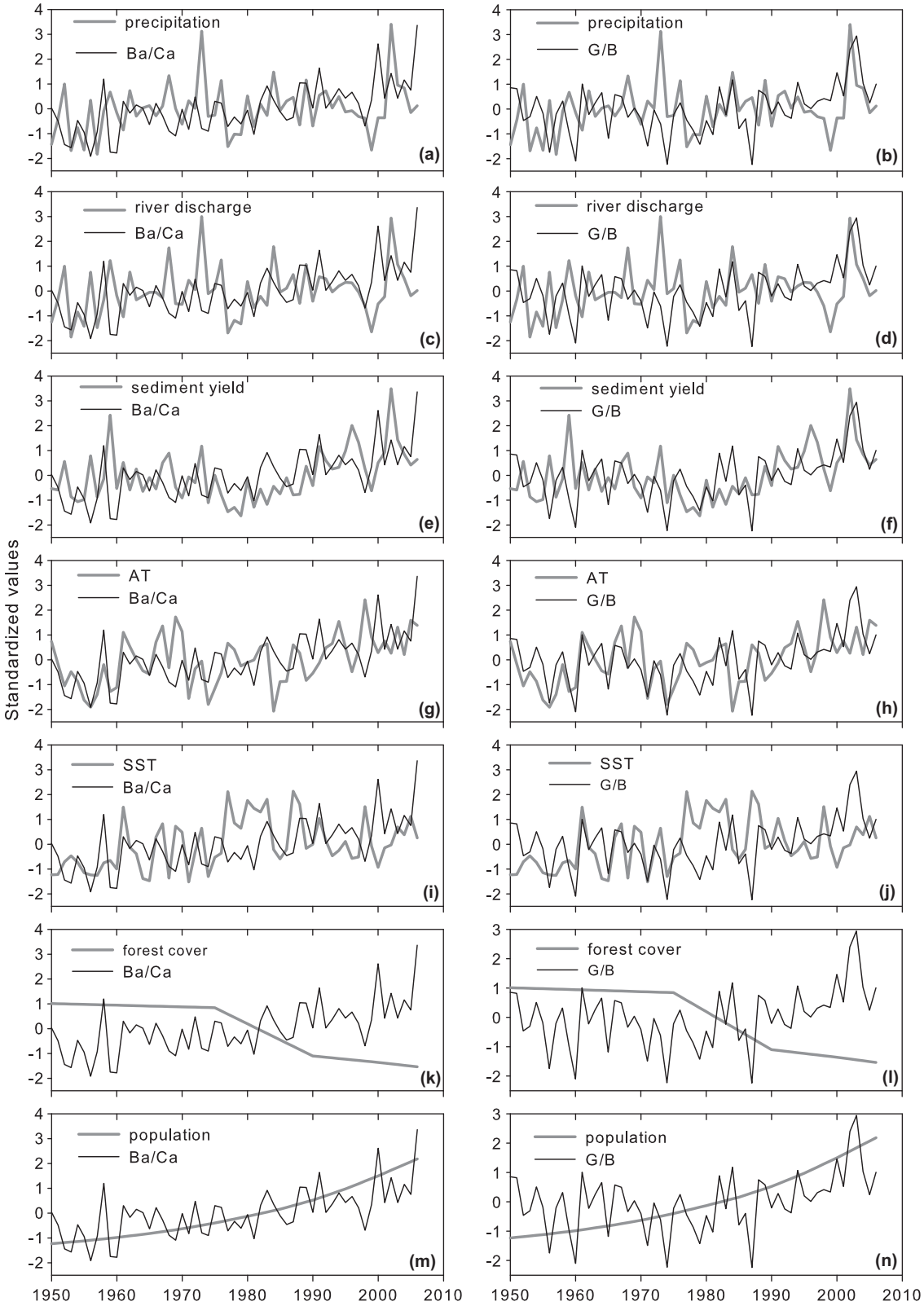

Fig. 4. Annual standardized time series of environmental variables and coral proxies for the NE. The grey line is an environmental variable, while the thin line is a Ba/Ca or G/B repeated on all plots. The two coral Ba/Ca, and G/B time series were averaged by calculating the arithmetic mean of the standardized time series.

Please cite this article in press as: Maina, J., et al. Linking coral river runoff proxies with climate variability, hydrology and land-use in Madagascar catchments. Mar. Pollut. Bull. (2012), http://dx.doi.org/10.1016/j.marpolbul.2012.06.027

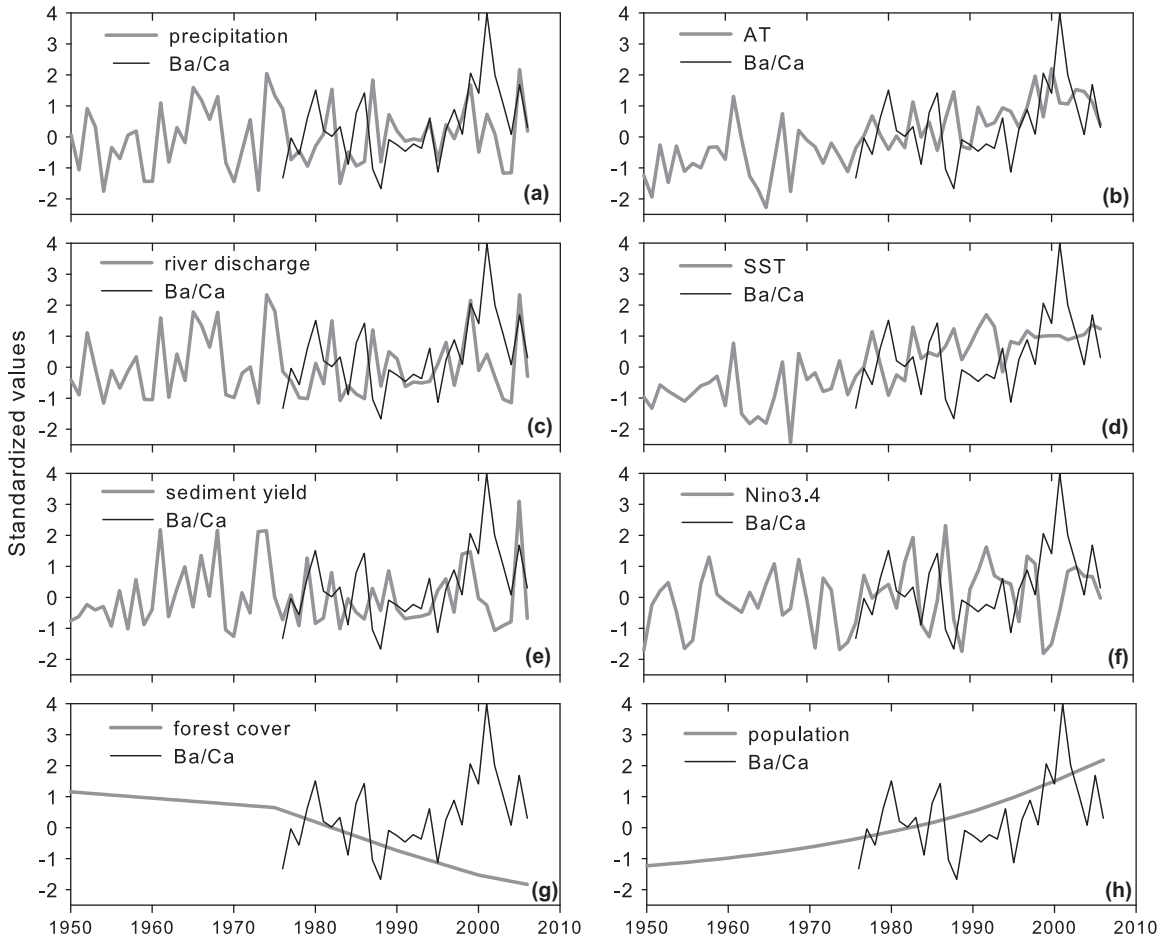

Fig. 5. Annual standardized time series of environmental variables and coral proxies for the SW. The grey line is an environmental variable, while the thin line is a Ba/Ca repeated on all plots. The two coral Ba/Ca time series were averaged by calculating the arithmetic mean of the standardized time series.

increasing trend while a declining trend is observed for forest cover (Figs. 4 and 5). In the SW, PC 1 showed step-like positive changes during 1969, 1977, 1987, and 1997 (Fig. 3f). The last two change points approximately corresponded with those depicted by the trends in the two coral proxies in 1989 and 1999 (Fig. 3i and j). The positive step like change in PC1 represents an increasing trend for temperature and population growth and a decrease in forest cover.

3.3. Seasonal variability in observational, modeling and coral data

Fig. 6 illustrates the seasonal dynamics of the modeled discharge, the coral proxies and several other environmental indicators for both catchments. Visual inspection of the seasonal dynamics indicates high synchrony among the hydrological variables (Fig. 6a and b), precipitation and discharge, and between the two regions, with peak values during the wet season between January and March and lowest values in the dry season between September and October (Fig. 6a and b). Climatic differences between the NE and SW in hydrological variables are also evident. During wet months, precipitation and discharge is higher in the NE than in the SW (Fig. 6a and b). The NE is wet throughout the year with relatively high discharge. The discharge in the SW shows a sharp peak around February whereas peak discharge in the NE is more evenly distributed throughout the rainy season (Fig. 6b). AT and SST showed an almost similar seasonal timing as hydrological variables: the highest temperatures occurred between January and March and the lowest temperatures between August and September (Fig. 6e and f). The average SSTs of the warmest and coldest months in the NE region were higher than in the subtropical SW region, which has higher temperature variability than the NE. From October to March, AT is higher in the SW than the NE (Fig. 6f).

Coral Ba/Ca (for NE and SW cores) and G/B (for NE cores only) show a seasonal pattern of high values between January and April, which were also the wettest and warmest months of the year with high rainfall/discharge (Fig. 6c and d). Coral proxy signals were lowest for September and October in the NE and SW consistent with the peak dry season in hydrological variables. The contrast between the wet and dry season in Ba/Ca is strongest for the GRT1 core in the SW (Fig. 6c). The G/B ratio (only available for the NE cores) displays a more pronounced seasonal signal (Fig. 6d). Overall, the seasonal signals of both coral proxies are in line with the seasonal discharge and precipitation patterns. Ba/Ca and G/B signals remain relatively high for the months following the peak discharge. Proxy signal differences between the NE and SW were also evident. Ba/Ca signals observed in the SW were higher than in the NE during the peak runoff season (Fig. 6c).

Autocorrelograms for hydrological variables, precipitation, temperature, and coral proxies clearly showed a pronounced sine-like waveform and correlation coefficients (secondary *y*-axis) that attain a minimum at a lag of 6 months and a maximum at lags 1 and 12, typical of annual seasonal cycle (Fig. 6, right panel). The maximum value of the graphed autocorrelation coefficient (R), when statistically significant, indicates the periodicity of the time series. All R-values were significant, indicating high similarity within respective months. Pairwise Pearson's correlation coeffi-

Please cite this article in press as: Maina, J., et al. Linking coral river runoff proxies with climate variability, hydrology and land-use in Madagascar catchments. Mar. Pollut. Bull. (2012), http://dx.doi.org/10.1016/j.marpolbul.2012.06.027

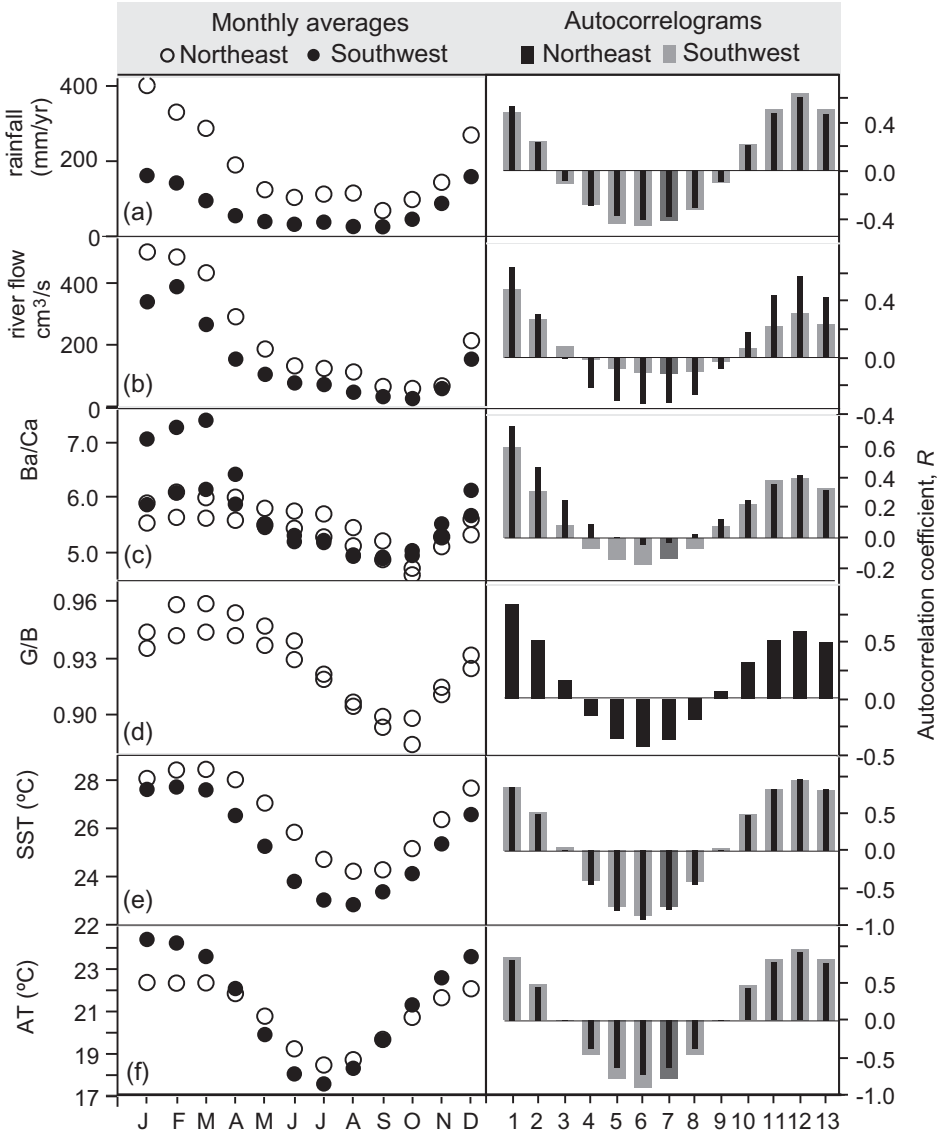

Fig. 6. Average seasonal cycles of environmental parameters and coral geochemical proxies for NE and SW regions in Madagascar. Note that G/B (panel d) is only available for NE. Panels on the right are the autocorrelograms for each variable, with autocorrelation coefficients indicated on the secondary *y*-axis. Thirteen periods are shown on the autocorrelograms to illustrate that maximum value occurs at period 12 indicating an annual seasonal cycle and periodicity of the time series.

cients between individual cores (G/B, Ba/Ca) and environmental variables are also reported in SI4.

Multiple regressions to investigate environmental drivers of coral proxies from the NE catchment indicate that precipitation, sediment load, and river flow (in this order of importance) best explained the yearly changes in Ba/Ca (Table 2). These results were obtained at $lag = t + 2$, as $lag = t + 0 \ldots t + 1$ yielded no significant results. When multiple regressions were repeated with G/B as the response variable, three variable combinations were found to significantly explain the yearly variability in G/B ($lag = t + 0$), sediment yield (interchangeably with precipitation and river flow), AT and ENSO (Table 2). In these three models, ENSO has a negative influence on G/B while sediment load and temperature showed a positive influence (Table 2). Regressions at $lags = t + 0 \ldots 1$ showed no significant results, while at $lag = t + 2$, only hydrological variables and precipitation significantly explained the variability of Ba/Ca (Table 2). In the warmer and drier SW catchment, AT and ENSO form a model that significantly explains the variability in Ba/Ca, having opposite effects (*at* $lag = t + 1$). Unlike in the NE, sediment yield and discharge do not significantly explain the variability of Ba/Ca. This is consistent with the PCA results using undetrended data, which showed a less dominant role of hydrological variables relative to temperature in the SW.

4. Discussion

We investigated the linkages between watershed characteristics (climate, land use, population, and hydrological variability), and environmental proxy records derived from coral skeletons (Ba/Ca and G/B) in NE and SW catchments of Madagascar, in the SW Indian Ocean. Previous studies have found correlation between precipitation, river discharge and suspended sediment load with the coral river runoff proxies (luminescence intensity, Ba/Ca), the concept underpinning reconstructions of historical rainfall, river flow and the amount of sediment in river flow (e.g., McCulloch et al., 2003; Lough, 2011). We analyzed for potential or likely association between these variables in Madagascar and investigated

Please cite this article in press as: Maina, J., et al. Linking coral river runoff proxies with climate variability, hydrology and land-use in Madagascar catchments. Mar. Pollut. Bull. (2012), http://dx.doi.org/10.1016/j.marpolbul.2012.06.027

possible causative roles of environmental drivers of changes that have occurred over the past five decades.

We confirm that in Madagascar catchments, precipitation, sediment load and river flow are associated with coral proxies from adjacent reefs at historical time scales, further extending the work of Grove et al. (2010, 2012) in the NE catchments. We established that the seasonal river discharge signal is well recorded in both Ba/Ca and G/B ratios, where coral proxies values remain elevated during several months after the peak discharge has occurred (Grove et al., 2012). This is possibly due to the time delay in plume dispersion and the incorporation of the proxies into the coral skeleton. Similar results were reported by Barnes and Lough (1993) and Jupiter (2006) for the Great Barrier Reef.

Results indicate, overall, that there is significant covariance between forest cover, population, river flow, sediment load, and the coral environmental proxies at annual and seasonal time scales. For the NE, changes in river discharge, sediment yield, precipitation, ENSO and temperature (AT, SST) were the main predictors of the variability in Ba/Ca and G/B; for the SW, changes in AT and ENSO were the significant predictors. Strong coral proxy signals were associated with increases in precipitation and hydrological indices (Table 2) in the NE. In both regions, while ENSO negatively influenced the variability in coral proxies, AT positively influenced the variability of Ba/Ca. Relationships between river discharge and coral proxy signals have been confirmed in other regions, (e.g., Jupiter, 2006; McCulloch et al., 2003; Prouty et al., 2010), but the role of temperature (AT, SST) and ENSO in determining such proxies has not been clearly established. Earlier studies (e.g., Lea et al., 1989; Shen et al., 1992; Fallon et al., 1999) have proposed, yet not verified, that the Ba distribution coefficient between coral and seawater is temperature dependent. Our study does confirm a causative role of temperature (AT, SST) and ENSO in both regions, albeit through different processes: NE corals may be responding to more extreme discharge, whereas in the SW coral Ba/Ca is responding directly to temperature (AT and/or SST) changes, which are directly sensitive to ENSO (Nicholson and Selato, 2000).

The hydrological variables (precipitation, discharge, sediment yield), and coral proxies for the NE were highly synchronized in terms of the long-term trends as revealed by the time series plots (Figs. 4 and 5) and by the PCA analyses (Table 1, Fig. 3). The increase in sediment yield since the late 1970s/early 1980's in the NE is also reflected in precipitation and river discharge, consistent with both coral Ba/Ca and G/B (Fig. 4). This adds confidence to our coral proxy reconstructions in terms of the changes in the long-term trends in sediment yield. We can confirm that the postulated increase in Ba/Ca and G/B by Grove et al. (2010) is indeed related to an overall increase in sediment yield.

In the SW, Ba/Ca indicates a lower baseline signal from the late 1980's to mid 1990's, and a sharp increase in late 1990's, possibly related to the wetter conditions following the dry 1997/98 El Niño year (Fig. 5) (Zhong et al., 2005). PCA revealed significant covariance of precipitation, sediment and discharge with only one core (GRT1). Further, the temporal trend of the averaged SW cores (Fig. 5) corresponds to those of sediment and discharge during the late 1980's and early 1990's, which was a relatively dry decade with low sediment yield and river discharge. Unlike in the NE, sediment yield, discharge and precipitation did not significantly explain Ba/Ca variability in the two SW cores. However, given that ENSO explained the Ba/Ca variability in this region (Table 2) and its known influence on precipitation (Nicholls, 1988), a role of precipitation and hydrology on Ba/Ca changes can still be inferred for this region.

The seemingly lack of explanatory power by the hydrology and precipitation in the SW may be explained by the vast extent of the SW watershed, which ranges from the eastern mountains with annual rainfall of 1200 mm, to the lowland coastal plains with only 100 mm (Fig. 1). The rivers Onilahy and Fiherenana, which drain the SW watershed, originate from the eastern plateaus and transport sediment loads even when most of the SW region is dry. The Onilahy River is likely the most important source of sediments reaching the GRT, due to the main direction of southerly winds that distribute the river plumes northwards. The SW reefs have a complex and shallow architecture, with large intertidal zones. These provide ideal conditions for resuspension of fine sediments, driven by the strong tidal currents, sea winds and the frequent cyclones (Bruggemann et al., accepted for publication). In contrast, cores from the NE are from a reef with a much simpler structure, in form of a shallow fringing reef surrounding a small island and directly exposed to the river plume that disperses towards that fringing reef. Given that the NE and SW regions are prone to frequent storms and cyclones (Nassor and Jury, 1998), sediment resuspension could lead to 'committed sedimentation' from accumulation of the past sediment deposits whose signals can be recorded by corals at the time of resuspension, even when there is no rainfall or new deposition (Jupiter et al., 2008; Prouty et al., 2010). Resuspension of sediments could be a secondary source of dissolved Ba for the corals in the SW enhancing Ba/Ca seasonality, and may contribute to temporal mismatch and lack of correlation between hydrology and proxy signals. Coral Ba/Ca in areas not influenced by terrestrial discharge are known to display seasonal signals that have been related to seasonal upwelling (Tudhope et al., 1996; Lea et al., 1989), which can be generated by zonal winds that are influenced by ENSO cycles (Fallon et al., 1999). However, upwelling as a secondary driver of high Ba/Ca seasonality in the SW is not supported by recent monitoring data for the same region (Bruggemann et al., accepted for publication).

We observed mismatches between the interannual variability in either river discharge or sediment load and coral runoff proxies (Figs. 4 and 5). These were also evident in the GLM's where predictor variables performed better with the introduction of 1–2 year lags (Table 2), indicating possible alignment errors in the time series data and/or physical process in the hinterland and differences in local environmental influences. Similar results were observed for the Great Barrier Reef (McCulloch et al., 2003), e.g., when dry years were followed by wet years, the erosive potential increased due to the loss of groundcover. Consequently increased suspended sediment loads and elevated coral Ba/Ca signals were observed even in years with average precipitation and river discharge (McCulloch et al., 2003). Examples in our coral proxy data time series in the NE (Fig. 4) include the dry mid 1950s which was followed by wet years in late 1950s leading to a spike in sediment load, and the dry 1997/1998 period which was followed by a relatively wet period and high sediment yield. These drought-breaking rain and floods that increase sediment discharge can distort the otherwise linear relationship between river discharge, sediment yield and coral proxy signals. Similarly, consecutive wet years result in lower erosion due to the soil saturation and subsequently low runoff proxy signals during wet years (Alibert et al., 2003; McCulloch et al., 2003). Our results for the NE and SW catchments show evidence for non-linear relationships between precipitation and sediment yield on inter-annual, decadal and longer time scales (Figs. 4 and 5).

The timing of the change points in environmental variables (NE: 1958, 1991, 2002; SW: 1987, 1997) did roughly correspond to those observed in river runoff proxies (NE: 1958, 1988, 2000; SW: 1989, 1999), although within 2–3 years lag times in response to environmental changes (Figs. 4 and 5). These alignment errors can also be due to uncertainties from proxy dating; time averaging of proxy signals with skeletal growth; and catchment soil moisture characteristics. Coincidentally, the years 1977, 1982, 1987, 1991, 1997, and 2002 were strong El Niño years, while 2000 was a La Niña year (Chen et al., 2004). It appears that some of the significant

Please cite this article in press as: Maina, J., et al. Linking coral river runoff proxies with climate variability, hydrology and land-use in Madagascar catchments. Mar. Pollut. Bull. (2012), http://dx.doi.org/10.1016/j.marpolbul.2012.06.027

change points are associated with ENSO, further highlighting the role of ENSO on tropical coastal ecosystems in the western Indian Ocean (Zinke et al., 2004, 2005).

Indeed, the tropical Pacific imparts substantial climate variability to the western Indian Ocean (Zinke et al., 2005), where the warm phase of ENSO is associated with droughts, while the cold phase is associated high rainfall (Zhong et al., 2005). ENSO's indirect influence on rainfall has been shown to occur most consistently in south-western Africa (15–32°S) (Nicholson and Selato, 2000; Zhong et al., 2005). The ENSO/rainfall relationships are manifestations of the influence of ENSO on these Indian and Atlantic oceans (Nicholson, 1997; Goddard and Graham, 1999; Nicholson et al., 2001). During the first half of La Nina episodes (warm phase), there is a tendency for anomalously dry conditions. As with El Nino, the La Nina signal is strongest during the second half of the episode (cold phase), but in contrast to El Nino, the rainfall is abnormally high (Nicholson and Selato, 2000).

Our results show that in both regions, the ENSO cycle is an important factor in explaining the variability of coral runoff proxies (G/B in the NE; Ba/Ca in SW) (Table 2). Given that ENSO is not highly correlated with rainfall (Table 1), it appears that ENSO influence is most significant during extreme high or low runoff in specific years that are associated with either phases of the ENSO. Similarly, Ward et al. (2010) found that ENSO has a greater impact on extreme discharge years than on years with mean annual discharge. ENSO variations have been shown to correlate with discharge in many parts of America, Australia, northern Europe, and parts of Africa and Asia (Dettinger et al., 2000), reinforcing the postulation that global weather patterns captured by the ENSO have a significant forcing on both stream-flows and coastal ecosystems around the world (Ward et al., 2010). Recent work in Madagascar (Ingram and Dawson, 2005) and in continental Africa (Anyamba et al., 2001) showed a negative influence of ENSO on vegetation cover. Further, Zinke et al. (2004) showed evidence for the influence of ENSO on SST in the nearby Ifaty lagoon in the SW of Madagascar, where ENSO years after the 1970's were characterized by high SST and low rainfall. This is consistent with our GLM results, which showed a negative impact of ENSO on coral Ba/Ca in the SW.

Overall, our results corroborate the hypothesis that there are strong linkages between watersheds' climate variability, hydrology, forest cover, population growth and the adjacent coral reefs. Changes in forest cover in the respective watersheds and population size were not directly connected to coral runoff proxies, and they did not significantly predict the variability in coral proxy signals in both regions as shown by the regression models. They did however highly co-vary with coral runoff signals and with the hydrological variables. This suggests that changes in land use and increased population density might govern the long-term trends in sediment yield and coral environmental proxy data, but that these are slow processes. They interact with climatic changes through precipitation to influence the amount of sediment transported through river runoff, which is subsequently deposited in coastal waters and reflected in elevated Ba/Ca and G/B in corals. This reinforces the need to incorporate terrestrial land use management in the design of coral reef protection networks.

Acknowledgements

This work was funded by the Western Indian Ocean Marine Science Association through the Marine Science for Management program (MASMA/OR/2007/02 and MASMA/CC/2010/02). The Macquarie University's Higher Degree Research program provided a PhD scholarship to J. Maina. The Wildlife Conservation Society (WCS) Madagasacar, Mr. BemahafalyRandriamanantsoa, and the WCS/ANGAP team in Maroantsetra, provided logistical support during fieldwork and assistance in obtaining research permits. CAF/CORE Madagascar granted with the CITES permit. ANGAP Madagascar helped with fieldwork in the vicinity of the marine and forest nature parks in Antongil Bay. Prof. M.T. McCulloch and Dr. S. Eggins from ANU Canberra assisted with the Laser Ablation ICP-MS measurements. Dr. K.P. Jochum provided access to the ICP-MS facilities of the Max-Planck-Institut für Chemie, Mainz (Germany) where measurements on the SW Madagascar cores were carried out. Bob Koster and Rineke Gieles continuously develop and maintain the UV-Core Scanner at Royal NIOZ.

Appendix A. Supplementary data

Supplementary data associated with this article can be found, in the online version, at http://dx.doi.org/10.1016/j.marpolbul.2012.06.027.

References

Anyamba, A., Tucker, C.J., Eastman, J.R., 2001. NDVI patterns over Africa during the 1997/1998 ENSO warm events. International Journal of Remote Sensing 22, 1847–1859.

Aerts, J.C.J.H., Kriek, M., Schepel, M., 1999. STREAM, spatial tools for river basins and environment and analysis of management options: 'set up and requirements'. Physics and Chemistry of the Earth, Part B 24, 591–595.

Aerts, J.C.J.H., Bouwer, L.M., 2002. Calibration and validation for the wider Perfume River Basin in Vietnam. Commissioned report and guided by R. Misdorp RIKZ/Coastal Zone Management Centre, The Hague, 35p.

Alibert, C., Kinsley, L., Fallon, S.J., McCulloch, M.T., Berkelmans, R., McAllister, F., 2003. Source of trace element variability in Great Barrier Reef corals affected by the Burdekin flood plumes. Geochimicaet Cosmochimica Acta 67 (2), 231–246.

Alory, G., Wijffels, S., Meyers, G., 2007. Observed temperature trends in the Indian Ocean over 1960–1999 and associated mechanisms. Geophysical Research Letters 34, L02606.

Barnes, D.J., Lough, J.M., 1993. On the nature and causes of density banding in massive coral skeleton. Journal of Experimental Marine Biology and Ecology 167, 91–108.

Box, G.E.P., Jenkins, G.M., 1976. Time SeriesAnalysis: Forecasting and Control (revised edition). Holden Day, San Francisco.

Bouwer, L.M., Aerts, J.C.J.H., Droogers, P., Dolman, A.J., 2006. Detecting the long-term impacts from climate variability and increasing water consumption on runoff in the Krishna river basin (India). Hydrology and Earth System Science 10, 703–713.

Bruggemann, J.H., Rodier, M., Guillaume, M.M.M., Andrefouet, S., Arfi, R., Cinner, J., et al. Wicked social-ecological problems forcing unprecedented change on the latitudinal margins of coral reefs: the case of southwest Madagascar. Ecology and Society, accepted for publication.

Carpenter, S.R., Cole, J.J., Pace, M.L., Batt, R., Brock, W.A., Cline, T., Coloso, J., Hodgson, J.R., Kitchell, J.F., Seekell, D.A., Smith, L., Weidel, B., 2011. Early warnings of regime shifts: a whole-ecosystem experiment. Science 332, 1079–1082.

Chabanet, P., Adjeroud, M., Andrefouet, S., Bozec, Y.-M., Garcia-Chanton, J.-A., Schrimm, M., 2005. Human-induced physical disturbance and their indicators on coral reef habitats: a multi-scale approach. Aquatic and Living Resources 18, 215–230.

Chatfield, C., 2004. The Analysis of Time Series – An Introduction, sixth ed. Chapman and Hall, London, UK.

Chen, D., Cane, M.A., Kaplan, A., Zebiak, S.E., Huang, D., 2004. Predictability of El Niño over the past 148 years. Nature 428, 733–734.

Cranet, T.A., Surle, G.A., 2002. Model-dependent variance inflation factor cutoff values. Quality Engineering 14, 391–403.

Darling, E.S., McClanahan, T.R., Cote, I.M., 2010. Combined effects of two stressors on Kenyan coral reefs are additive or antagonistic, not synergistic. Conservation Letters 3, 122–130.

Davis, J.C., 1986. Statistics and Data Analysis in Geology, second ed. John Wiley and Sons, New York, 646p.

Dettinger, M.D., Cayan, D.R., McCabe, G.J., 2000. Multiscale streamflow variability associated with El Niño/Southern Oscillation. In: Diaz, H.F., Markgraf, V. (Eds.), El Niño and the Southern Oscillation: Multiscale Variability and Global and Regional Impacts. Cambridge Univ. Press, Cambridge, U.K, pp. 113–147.

Durbin, J., Watson, G.S., 1971. Testing for serial correlation in least squares regression III. Biometrika 58, 1–19.

Eakin, C.M., Lough, J.M., Heron, S.F., 2009. Climate, weather and coral bleaching. In: van Oppen, M.J.H., Lough, J.M. (Eds.), Coral Bleaching: Patterns, Processes, Causes and Consequences. Springer, New York, pp. 41–67.

Eslinger, D.L., Carter, H.J., Dempsey, E., VanderWilt, M., Wilson, B., Meredith, A., 2005. The Nonpoint-Source Pollution and Erosion Comparison Tool. NOAA Coastal Services Center, Charleston, South Carolina. <http://www.csc.noaa.gov/nspect/> [accessed xx.7.2011].

Fabricius, K.E., Langdon, C., Uthicke, S., Humphrey, C., Noonan, S., De'ath, G., Remy Okazaki, R., Muehllehner, N., Glas, M.S., Lough, J.M., 2011. Losers and winners in

coral reefs acclimatized to elevated carbon dioxide concentrations. Nature Climate Change. http://dx.doi.org/10.1038/NCLIMATE1122.
Fallon, S.J., McCulloch, M.T., van Woesik, R., Sinclair, D.J., 1999. Corals at their latitudinal limits: laser ablation trace element systematics in Porites from Shirigai Bay, Japan. Earth Planetary Science Letters 172, 221–238.
Fallon, S.J., White, J.C., McCulloch, M.T., 2002. *Porites* corals as a recorder of mining and environmental impacts: Misima Island, Papua New Guinea. Geochimica et Cosmochimica Acta 66, 45–62.
FAO/IIASA/ISRIC/ISSCAS/JRC, 2009. Harmonized World Soil Database (version 1.1). FAO, Rome, Italy and IIASA, Laxenburg, Austria.
Felis, T., Pätzold, J., 2003. Climate records from corals. In: Wefer, G., Lamy, F., Mantoura, F. (Eds.), Marine Science Frontiers for Europe. Springer, New York, pp. 11–27.
Gardner, T.A., Cote, I.M., Gill, J.A., Grant, A., Watkinson, A.R., 2003. Long-term region-wide declines in Caribbean corals. Science 301, 958–960.
Goddard, L., Graham, N.E., 1999. Importance of the Indian Ocean for simulating rainfall anomalies over eastern and southern Africa. Journal of Geophysical Research 104, 19 099–19 116.
Grottoli, A.G., Eakin, C.M., 2007. A review of modern coral d18O and d14C proxy records. Earth-Science-Reviews 81, 67–91.
Grove, C.A., Zinke, J., Scheufen, T., Maina, J., Epping, E., Boer, W., Randriamanantsoa, B., Brummer, G.J.A., 2012. Spatial linkages between coral proxies of terrestrial runoff across a large embayment in Madagascar. Biogeosciences Discussion 9, 3099–3144.
Grove, C.A., Nagtegaal, R., Zinke, J., Scheufen, T., Koster, B., Kasper, S., McCulloch, M.T., van den Bergh, G., Brummer, G.J.A., 2010. River runoff reconstructions from novel spectral luminescence scanning of massive coral skeletons. Coral Reefs 29, 579–591.
Habeeb, L.R., Trebilko, J., Wotherspoon, S., Johnson, C.R., 2005. Determining natural scales of ecological systems. Ecological Monographs 75, 467–487.
Hannah, L., Dave, R., Lowry, P., Andelman, S., Andrianarisata, M., Andriamaro, L., Cameron, A., Hijmans, R., Kremen, C., MacKinnon, J., Randrianasolo, H.H., Andriambololonera, S., Razafimpahanana, A., Randriamahazo, H., Randrianarisoa, J., Razafinjatovo, P., Raxworthy, C., Schatz, G.E., Tadross, M., Wilmé, L., 2008. Climate change adaptation for conservation in Madagascar. Biology Letters 4, 590–594.
Harper, G.J., Steininger, M.K., Tucker, C.J., Juhn, D., Hawkins, F., 2007. Fifty years of deforestation and forest fragmentation in Madagascar. Environmental Conservation 34, 325–333.
Harris, A., Manahira, G., Sheppard, A., Gough, C., Sheppard, C., 2010. Demise of Madagascar's once Great Barrier Reef – change in coral reef condition over 40 years. Atoll Research Bulletin 574.
Hoegh-Guldberg, O., Mumby, P.J., Hooten, A.J., Steneck, R.S., Greenfield, P., Gomez, E., Harvell, C., Sale, P.F., Edwards, A.J., Caldeira, K., Knowlton, N., Eakin, C.M., Iglesias-Prieto, R., Muthiga, N., Bradbury, R.H., Dubi, A., Hatziolos, M., 2007. Coral reefs under rapid climate change and ocean acidification. Science 318, 1737–1742.
Hofmann, J., Behrendt, H., Gilbert, A., Janssen, R., Kannen, A., Kappenberg, J., Lenhart, H., Lise, W., Nunneri, C., Windhorst, W., 2005. Catchment-coastal zone interaction based upon scenario and model analysis: Elbe and the German Bight case study. Regional Environmental Change 5, 54–81.
Ingram, J.C., Dawson, T.P., 2005. Climate change impacts and vegetation response on the island of Madagascar. Philosophical Transactions of the Royal Society 363, 55–59.
Isdale, P.J., Stewart, B.J., Tickle, K.S., Lough, J.M., 1998. Palaeohydrological variation in a tropical river catchment: a reconstruction using fluorescent bands in corals of the Great Barrier Reef, Australia. The Holocene 8, 1–8.
Jackson, J.E., 2003. A Users Guide to Principal Components. Wiley, Hoboken.
Jolliffe, I.T., 2004. Principal Component Analysis. Springer, New York, USA.
Jupiter, S.D., 2006. From cane to coral reefs: ecosystem linkages and downstream responses to land use intensification. Ph.D. Thesis, University of California, Santa Cruz, 300pp.
Jupiter, S., Roff, G., Marion, G., Henderson, M., Schrameyer, V., McCulloch, M., Hoegh-Guldberg, O., 2008. Linkages between coral assemblages and coral proxies of terrestrial exposure along a cross-shelf gradient on the southern Great Barrier Reef. Coral Reefs 27, 887–903.
Jury, M.R., Pathak, B., 1991. A study of climate and weather variability over the tropical Southwest Indian Ocean. Meteorology and Atmospheric Physics 47, 37–48.
Kuleshov, Y., Qi, L., Fawcett, R., Jones, D., 2008. On tropical cyclone activity in the Southern Hemisphere: trends and the ENSO connection. Geophysical Research Letters, 35, L14S08, http://dx.doi.org/10.1029/2007GL032983.
Lea, D.W., Shen, G.T., Boyle, E.A., 1989. Coralline barium re-cords temporal variability in equatorial Pacific upwelling. Nature 340, 373–376.
Lehner, B., Verdin, K., Jarvis, A., 2008. New global hydrography derived from space borne elevation data. Eos, Transactions, AGU 89, 93–94.
Lewis, S.E., Brodie, J.E., McCulloch, M.T., Mallela, J., Jupiter, S.D., Williams, H.S., Lough, J.M., Matson, E.G., 2011. An assessment of an environmental gradient using coral geochemical records, Whitsunday Islands, Great Barrier Reef, Australia. Marine Pollution Bulletin. http://dx.doi.org/10.1016/j.marpolbul.2011.09.030.
Lindenmayer, D.B., Hobbs, R.J., Likens, G.E., Krebs, C.J., Banks, S.C., 2011. Newly discovered landscape traps produce regime shifts in wet forests. Proceedings of the National Academy of Sciences of the United States of America 108, 15887–15891.
Lough, J.M., Barnes, D.J., McAllister, F.A., 2002. Luminescent lines in corals from the Great Barrier Reef Provide spatial and temporal records of reefs affected by land runoff. Coral reefs 21, 333–343.
Lough, J.M., 2011. Great Barrier Reef coral luminescence reveals rainfall variability over northeastern Australia since the 17th century. Paleoceanography 26. http://dx.doi.org/10.1029/2010PA002050.
Lu, H., Moran, C.J., Prosser, I.P., 2006. Modelling sediment delivery ratio over the Murray Darling Basin. Environmental Modelling& Software 21, 1297–1308.
Lui, G.C.S., Li, W.K., Leung, K.M.Y., Lee, J.H.W., Jayawardena, A.W., 2007. Modelling algal blooms using vector autoregressive models with exogenous variables and long memory filter. Ecological Modelling, 130–138.
Mansfield, E.R., Helms, B.P., 1982. Detecting multicollinearity. The American Statistician 36, 158–160.
Mavume, A.F., Rydberg, L., Rouault, M., Lutjeharms, J.R.E., 2000. Climatology and landfall of tropical cyclones in the south-west Indian Ocean. Western Indian Ocean Journal of Marine Science 8, 15–36.
McCulloch, M., Fallon, S., Wyndham, T., Hendy, E., Lough, J., Barnes, D., 2003. Coral record of increased sediment flux to the inner Great Barrier Reef since European settlement. Nature 421, 727–730.
Mertz-Kraus, R., Brachert, T.C., Jochum, K.P., Reuter, M., Stoll, B., 2009. LA-ICP-MS analyses on coral growth increments reveal heavy winter rain in the Eastern Mediterranean Ma. Palaeogeography, Palaeoclimatology, Palaeoecology 273, 25–40.
Mitchell, T.D., Jones, P.D., 2005. An improved method of constructing a database of monthly climate observations and associated high-resolution grids. International Journal of Climatology 25, 693–712.
Mora, C., 2010. A clear human footprint in the coral reefs of the Caribbean. Proceedings of Royal Society 275, 767–773.
Moriasi, D.N., Arnold, J.G., Van Liew, M.W., Bingner, R.L., Harmel, R.D., Veith, T.L., 2007. Model evaluation guidelines for systematic quantification of accuracy in watershed simulations. Transactions of the ASABE 50, 885–900.
Mumby, P.J., Dahlgren, C., Harborne, A.R., Kappel, C.V., Micheli, F., Brumbaugh, D.R., Holmes, K.E., Mendes, J.M., Broad, K., Sanchirico, J.N., Buch, K., Box, S., Stoffle, R.W., Gill, G.A., 2006. Fishing, trophic cascades, and the process of grazing on coral reefs. Science 311, 98–101.
Nam, P.T., Yang, D., Kanae, S., Oki, T., Musiake, K., 2003. Global soil loss estimates using rusle model: the use of global spatial dataset on estimating erosive parameters. Geoinformatics 14, 49–53.
Nash, J.E., Sutcliffe, J.V., 2004. River flow forecasting through conceptual models part I: a discussion of principles. Journal of Hydrology 10, 282–290.
Nassor, A., Jury, M.R., 1998. Intra-seasonal climate variability of Madagascar. Part 1: mean summer conditions. Meteorology and Atmospheric Physics 65, 31–41.
Nicholls, N., 1988. El Niño-Southern Oscillation and rainfall variability. Journal of Climate 1, 418–421.
Nicholson, S.E., 1997. On the characteristics of warm episodes in the tropical Atlantic and Indian Oceans. International Journal of Climatology 17, 345–375.
Nicholson, S.E., Selato, J.C., 2000. The influence of La Nina on African rainfall. Journal of Climatology 20, 1761–1776.
Nicholson, S.E., Leposo, D., Grist, J.R., 2001. On the relationship between El Nino and drought over Botswana. Journal of Climate 14, 323–335.
Paillard, D., Labeyrie, L., Yiou, P., 1996. Macintosh program performs time-series analysis. Eos 77, 379.
Pandolfi, J.M., Connolly, S.R., Marshall, D.J., Cohen, A., 2011. Projecting coral reef futures under global warming and ocean acidification. Science 333, 418–422.
Prouty, N.G., Field, M.E., Stock, J.D., Jupiter, S.D., McCulloch, M., 2010. Coral Ba/Ca records of sediment input to the fringing reef of the southshore of Moloka'i, Hawai'i over the last several decades. Marine Pollution Bulletin 60, 1822–1835.
Richmond, R.H., Rongo, T., Golbuu, T., Victor, S., Idechong, N., Davis, G., Kostka, W., Neth, L., Hamnett, M., Wolanski, E., 2007. Watersheds and coral reefs: conservation science, policy, and implementation. Bioscience 57, 598–607.
Rodionov, S.N., 2004. A sequential algorithm for testing climate regime shifts. Geophysical Research Letters 31, L09204.
Sinclair, D.J., McCulloch, M.T., 2004. Corals record low mobile barium concentrations in the Burdekin River during the 1974 flood: evidence for limited Ba supply to rivers? Palaeogeography 214, 155–174.
Shen, G.T., Cole, J.E., Lea, D.W., Linn, L.J., McConnaughey, T.A., Fairbanks, R.G.,1992. Surface ocean variability at Galapagos from 1936–1982: Calibration of geochemical tracers in corals. Paleoceanography 7, 563–588.
Sussman, W., Green, G.M., Sussman, L.K., 1994. Satellite imagery, human ecology, anthropology, and deforestation. Human Ecology 22.
Tudhope, A.W., Lea, D.W., Shimmield, G.B., Chilcott, C.P., Head, S., 1996. Monsoon climate and Arabian sea coastal upwelling recorded in massive corals from southern Oman. Palaios 11, 347–361.
Vorosmarty, C.J., Fekete, B.M., Tucker, B.A., 1998. Global River Discharge, 1807–1991, version. 1.1 (RivDIS). Data set. Available on-line <http://www.daac.ornl.gov> from Oak Ridge National Laboratory Distributed Active Archive Center, Oak Ridge, Tennessee, USA http://dx.doi.org/10.3334/ORNLDAAC/199.
Vrieling, A., Sterk, G., Jong, S.M.D., 2010. Satellite-based estimation of rainfall erosivity for Africa. Journal of Hydrology 395, 235–241.
Ward, P.J., Beets, W., Bouwer, L.M., Aerts, J.C.J.H., Renssen, H., 2010. Sensitivity of river discharge to ENSO. Geophysical Research Letters 37, L12402. http://dx.doi.org/10.1029/2010GL043215, 2010.
Wilkinson, C. (Ed.), 2004. Status of Coral Reefs of the World, Australian Institute of Marine Science, Townsville, Australia.

Please cite this article in press as: Maina, J., et al. Linking coral river runoff proxies with climate variability, hydrology and land-use in Madagascar catchments. Mar. Pollut. Bull. (2012), http://dx.doi.org/10.1016/j.marpolbul.2012.06.027

Zhang, X., Zwiers, F.W., Hegerl, G.C., Lambert, F.H., Gillett, N.P., Solomon, S., Stott, P.A., Nozawa, T., 2007. Detection of human influence on twentieth-century precipitation trends. Nature 448, 461–465.

Zhong, A., Hendon, H.H., Alves, O., 2005. Indian Ocean variability and its association with ENSO in a global coupled model. Journal of Climate 18, 3634–3649.

Zinke, J., Dullo, W.C., Heiss, G.A., Eisenhauer, A., 2004. ENSO and Indian Ocean subtropical dipole variability is recorded in a coral record off southwest Madagascar for the period 1659–1995. Earth and Planetary Science Letters 228, 177–194.

Zinke, J., Pfeiffer, M., Timm, O., Dullo, W.-C., Davies, G.R., 2005. Atmosphere-ocean dynamics in the western Indian Ocean recorded in corals. Philosophical Transactions of the Royal Society A 1826. http://dx.doi.org/10.1098/rsta.2004.1482.

Zuur, A.F., Tuck, I.D., Bailey, N., 2003. Dynamic Factor Analysis to estimate common trends in fisheries time series. Canadian Journal of fisheries and aquatic science 60, 542–552.

Zuur, A.F., Ieno, E.N., Walker, N., Saveliev, A.A., Smith, G.M., 2009. Mixed Effects Models and Extensions in Ecology with R, first ed. Springer, NY, USA.

Please cite this article in press as: Maina, J., et al. Linking coral river runoff proxies with climate variability, hydrology and land-use in Madagascar catchments. Mar. Pollut. Bull. (2012), http://dx.doi.org/10.1016/j.marpolbul.2012.06.027